

# Journal of Materials Chemistry B

Accepted Manuscript



This is an *Accepted Manuscript*, which has been through the Royal Society of Chemistry peer review process and has been accepted for publication.

*Accepted Manuscripts* are published online shortly after acceptance, before technical editing, formatting and proof reading. Using this free service, authors can make their results available to the community, in citable form, before we publish the edited article. We will replace this *Accepted Manuscript* with the edited and formatted *Advance Article* as soon as it is available.

You can find more information about *Accepted Manuscripts* in the [Information for Authors](#).

Please note that technical editing may introduce minor changes to the text and/or graphics, which may alter content. The journal's standard [Terms & Conditions](#) and the [Ethical guidelines](#) still apply. In no event shall the Royal Society of Chemistry be held responsible for any errors or omissions in this *Accepted Manuscript* or any consequences arising from the use of any information it contains.

# Gold Nanoparticle Labeling Based ICP-MS Detection/Measurement of Bacteria, and Their Quantitative Photothermal Destruction

Cite this: DOI: 10.1039/x0xx00000x

Yunfeng Lin and Ashton T. Hamme II\*

Received 00th January 2012,  
Accepted 00th January 2012

DOI: 10.1039/x0xx00000x

www.rsc.org/

**ABSTRACT:** Bacteria such as *Salmonella* and *E. coli* present a great challenge in public health care in today's society. Protection of public safety against bacterial contamination and rapid diagnosis of infection require simple and fast assays for the detection and elimination of bacterial pathogens. After utilizing *Salmonella DT104* as an example bacterial strain for our investigation, we report a rapid and sensitive assay for the qualitative and quantitative detection of bacteria by using antibody affinity binding, popcorn shaped gold nanoparticle (GNPOPs) labeling, surface enhanced Raman spectroscopy (SERS), and inductively coupled plasma mass spectrometry (ICP-MS) detection. For qualitative analysis, our assay can detect *Salmonella* within 10 min by Raman spectroscopy; for quantitative analysis, our assay has the ability to measure as few as 100 *Salmonella DT104* in a 1 mL sample (100 CFU/mL) within 40 min. Based on the quantitative detection, we investigated the quantitative destruction of *Salmonella DT104*, and the assay's photothermal efficiency in order to reduce the amount of GNPOPs in the assay to ultimately eliminate any potential side effects/toxicity to the surrounding cells *in vivo*. Results suggest that our assay may serve as a promising candidate for qualitative and quantitative detection and elimination of a variety of bacterial pathogens.

## 1. Introduction

Food borne pathogenic bacteria have consistently been a major threat to human health, and contamination of food by pathogenic bacteria such as *Salmonella* and *E. coli* have been a threat to human health throughout human history. *Salmonella Typhimurium DT104* is responsible in large part for salmonellosis in the United States.<sup>1</sup> A recent Centers for Disease Control and Prevention (CDC) report shows that an estimated 48 million illnesses, 128,000 hospitalizations, and 3,000 deaths of Americans occur each year were caused by pathogens in contaminated food.<sup>1, 2</sup> Every year, *Salmonella* is estimated to cause about 1.2 million illnesses in the United States, with about 23,000 hospitalizations and 450 deaths.<sup>3, 4</sup> *Escherichia coli* (*E. coli*) are members of a large group of bacterial strains that inhabit the intestinal tract of humans and other warm blooded animals, and as few as 10 cells can cause serious human illness and even death. The presence of *E. coli* in foodstuffs and drinking water is a chronic worldwide problem.<sup>5</sup>

There is an urgent need for reliable approaches to identify and eliminate harmful bacteria with high specificity and sensitivity.<sup>6-8</sup>

Department of Chemistry and Biochemistry, Jackson State University, 1400 J R Lynch street, Jackson, MS 39217, USA. E-mail: [ashton.t.hamme@jsums.edu](mailto:ashton.t.hamme@jsums.edu)

† Electronic supplementary information (ESI) available: Additional Experimental details, figures showing SERS scattering intensity change at 1590 cm<sup>-1</sup> upon the addition of different concentrations (CFU/mL) of bacteria, the temperature increase affected by the shape of different kinds of gold nanoparticles under laser, and the comparison of bacteria viability when GNPOP, round shape GNP and Gold nanorod conjugated with *Salmonella DT104* using 1 W/cm<sup>2</sup> 670 nm light for 30 min. See DOI: 10.1039/b000000x/

Various technologies have been developed for bacteria detection with regard to the optical, electrochemical, biochemical, and physical properties of microorganisms.<sup>9-12</sup> Traditional detection methods such as plating and culture usually involve time-consuming steps such as pre-concentration, and <sup>9, 13-15</sup> conventional techniques such as enzyme-linked immunosorbent assay (ELISA) and polymerase chain reaction (PCR) are limited due to cost and versatility constraints.<sup>16-24</sup> Moreover, bacteria like *Salmonella* have the ability to grow and survive in adverse environments (e.g., low nutrient concentrations and extreme temperatures as low as 5.9 °C and as high as 54 °C), and, as a result, *Salmonella* can propagate inside the human body.<sup>1, 3, 4, 25, 26</sup> In addition, once *Salmonella* enters into human body, worse diseases, such as hematosepsis, enteritis, can be induced.<sup>27-29</sup> Antibiotics have been an effective way to eliminate bacterial pathogens.<sup>30-32</sup> After the discovery of penicillin in 1940, antibiotics have been working as economic powerhouses for our society because they are the most effective antibacterial drugs for modern medical procedures.<sup>33-36</sup> However, bacterial pathogens are becoming drug-resistant due to the abuse of antibiotics worldwide.<sup>37, 38</sup> Furthermore, abuse of antibiotics can result in immeasurable side effects to normal cells.<sup>39-43</sup>

In this regard, the CDC/FDA (Food and Drug Administration) is encouraging efforts aimed at modernizing public health microbiology and bioinformatics capabilities to quicken microbial detection and response.<sup>4</sup> The development of new nanomaterials with multifunctional capabilities is extremely crucial for alleviating bacterial infections in their early stage.<sup>44</sup> Plasmonic gold nanoparticles (GNP) with optical properties that are tunable in the near-infrared (NIR) region are highly useful for biological imaging due to their high transmission rate through biological tissues.<sup>45-48</sup> In

addition, plasmatic gold nanotechnology has the potential to be a solution for treating multi-drug resistant bacteria (MDRB) infection and cancer, with high biocompatibility.<sup>49</sup> Various methods have been applied to attach antibodies to gold nanoparticles whereby selective binding with bacteria occurs through a specific antibody-antigen interaction. These methods include: 1) Linking the antibody to GNPOP directly, which takes advantage of the predominant glycosylation of the fragment crystallizable region of the antibody; 2) Linking the antibody to GNPOP by Cysteamine, which is known as the "glutaraldehyde spacer method"; 3) Linking the antibody to GNPOP by electrostatic interaction; and 4) Linking the antibody to GNPOP by Carboxy-PEG12-Thiol (PEG-SH).<sup>44, 50-52</sup> A variety of linkers, such as 4-aminothiophenol (4-ATP),<sup>53</sup> Cystamine,<sup>54</sup> 3-mercaptopropanoic acid,<sup>55</sup> 4-mercaptobenzoic acid,<sup>56</sup> Cysteine,<sup>57</sup> Dihydrolipoic acid (DHLLA),<sup>58</sup> and Glutathione<sup>59</sup> have also been effective bioconjugate linkers. The nanomaterial's high sensitivity and the use of Raman spectroscopy for highly informative spectra characteristics enable us to utilize surface-enhanced Raman spectroscopy (SERS) as a fingerprint for the detection of MDRB.<sup>38, 60</sup> Also, recently published articles from several groups,<sup>46, 61, 62</sup> including ours,<sup>44</sup> have demonstrated that GNPs of different sizes and shapes with tunable optical properties in the NIR region can be exploited for the hyperthermic photothermal destruction of bacteria, because GNPs have the ability to generate high temperatures at a desired site.<sup>38, 63, 64</sup>

Inductively coupled plasma mass spectrometry (ICP-MS) is one of the most sensitive techniques for trace element analysis, with a large dynamic range, low detection limits, and multi-element and rapid analysis capabilities.<sup>65-69</sup> Recently, the use of elemental tags and inorganic nanoparticles has also made ICP-MS amenable for the analysis of biomolecules.<sup>70, 71</sup> To carry out an analysis of the concentration of bacteria, an extra amount of the antibody-conjugated GNPs were added to a sample solution. The utilization of antibodies afforded a feasible way to specifically connect the bacteria and GNPs. After the mixture was centrifuged to separate the free GNPs from the mixture, GNPs bonded *Salmonella* was then acid-digested and the concentration of Au<sup>3+</sup> was quantified using ICP-MS. Standard curves were produced to correlate the concentration of *Salmonella DT104* and the concentration of Au<sup>3+</sup>. In the meantime, by determining the concentration of Au<sup>3+</sup> versus the concentration of *Salmonella*, the amount of GNPs (in the form of Au<sup>3+</sup>) could be correlated with each CFU of *Salmonella*.

Here, through utilizing *Salmonella enterica serovar Typhimurium definitive type 104* as an example, we report a qualitative and quantitative assay of popcorn shape gold nanoparticles (GNPOP) to detect bacteria by SERS and ICP-MS, and thereafter bacterial photothermal destruction, as shown in Figure 1. If *Salmonella DT104* is present in a sample, the low cross-section Raman signals of the GNPOPs assay could be amplified by several orders of magnitude, which is suitable for qualitative detection by SERS; also, The linear relationship between the concentration of *Salmonella* and GNPOPs enables our assay to be suitable for quick quantitative detection. Since *Salmonella* labeling and ICP-MS analysis require only minimum sample preparation, our assay is easy and fast. For qualitative analysis, our assay can detect *Salmonella* within 10 min by Raman spectroscopy; for quantitative analysis, our assay has the ability to measure as few as 100 *Salmonella DT104* in a 1 mL sample (100 CFU/mL) within 40 min.

Based on the ability of ICP-MS to perform concentration dependant measurements, our method will provide an evident benefit to photothermal therapy. For a given volume of bacteria, due to the fact

that the concentration of a given volume of bacteria can be detected through ICP-MS, an estimate can be made regarding the amount of GNPOPs needed for photothermal therapy. We found that in order to kill a specific concentration of bacteria we needed to increase the amount of GNPOPs to a concentration that is little higher than the calculated amount to reduce laser exposure time, and, to some extent, we can also seek a balance between the extra amount of GNPOPs and laser exposure time in order to optimize the bacteria destruction and minimize the negative side effects to the surrounding cells, which are especially meaningful and have great potential for *in vivo* applications. Also, results suggest that our assay may also serve as a promising candidate for qualitative and quantitative detection and elimination of a variety of bacterial pathogens.

Based on the SERS, ICP-MS and photothermal efficiency, GNPOP has some advantages compared to GNPs with other shapes. For SERS, the central sphere of GNPOPs can act as an electron reservoir, whereas the tips are capable of focusing the field at their apices.<sup>72</sup> Consequently, the sharp tips can provide a huge field enhancement of the SERS scattering signal.<sup>73</sup> For ICP-MS, when compared with normal sized spherical gold nanoparticles, the volume of the GNPOP is larger, which means each particle contains more Au atoms. Due to the fact that each bacteria has a limited number of antigen binding sites for the GNP-mAb hybrids,<sup>74</sup> the number of GNPs binding with each bacteria should be almost the same, regardless of the kind of GNP used. Therefore, binding with a larger sized GNPs means each bacterium will be attached to a large amount of Au atoms. Due to the fact that our detection is based on the Au signal from ICP-MS, which has a linear relationship with bacteria concentration below a certain range, the detection limit by using GNPOP will be lower than using spherical GNPs. For photothermal destruction, GNPOP also has a comparatively higher photothermal efficiency than spherical gold nanoparticles. One possible reason is that several narrow, nanoscale spikes in GNPOP were capable of focusing the field at their apices, which could provide considerable enhancement of photothermal efficiency.<sup>75</sup>

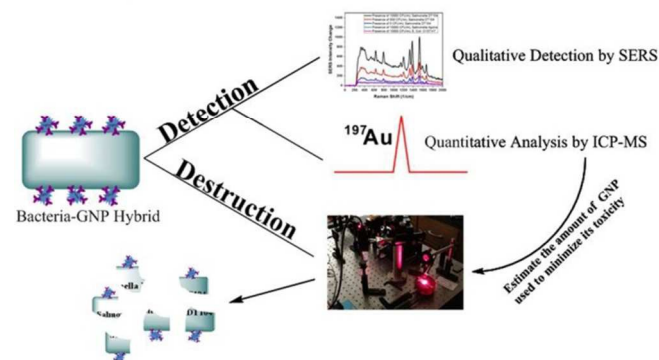


Figure 1. Schematic diagram showing the principle of our assay.

## 2. Experimental

### Chemicals and Materials

Hydrogen tetrachloroaurate (HAuCl<sub>4</sub> × 3H<sub>2</sub>O), sodium borohydride (NaBH<sub>4</sub>), silver nitrate (AgNO<sub>3</sub>), tri-sodium citrate (TSC), ascorbic acid (AA), cetyl trimethylammonium bromide (CTAB) were purchased from Sigma-Aldrich and used without further purification. Nanopure H<sub>2</sub>O was purchased from Fisher Scientific. Ampicillin, chloramphenicol, streptomycin, sulfonamides, and tetracycline antibiotic, multiple drug resistant (MDR) *Salmonella typhimurium DT104*, and other bacteria strains were obtained from the American

Type Culture Collection (ATCC, Rockville, MD; ATCC (700408). Monoclonal antibody (mAb) specific for *Salmonella DT104* was purchased from Abcam (Ab69238), and growth media for the bacteria were obtained from ATCC.

### Synthesis of Popcorn Shape Gold Nanoparticle (GNPOP)

Our GNPOP synthesis was achieved through a two-step process, using seed-mediated growth. In the first step, very small, reasonably uniform, spherical seed particles were generated using trisodium citrate as stabilizer and sodium borohydride as strong nucleating agent. In the second step, ascorbic acid was used as weak reductant, and CTAB was used as shape-templating surfactant, in order to ensure the seeds grew into larger particles of the particular morphology we desired. The ascorbic anions transfer electrons to the seed particles, resulting in the formation of a gold shell, which grows into different shapes in the presence of CTAB. Spherical gold seeds were synthesized by mixing aqueous solutions of hydrogen tetrachloroaurate (III) hydrate with trisodium citrate in 20 mL of double distilled deionized water (18 M $\Omega$ ), with a final concentration of  $2.5 \times 10^{-4}$  M for  $\text{HAuCl}_4 \cdot 3\text{H}_2\text{O}$  and  $10^{-4}$  M for trisodium citrate. An ice-cooled, freshly prepared aqueous solution of sodium borohydride ( $\text{NaBH}_4$ , 0.1 M, 60  $\mu\text{L}$ ), was then added under vigorous stirring. The solution turned pink immediately after the addition of  $\text{NaBH}_4$  and became red after it was kept in the dark overnight. The nanoseeds exhibited an absorption spectrum with a maximum at 510 nm, which corresponded to a 4.3 nm seed. It was also confirmed by TEM (JEOL, JEM 1011 electron microscope working at 100 kV equipped with a Gatan camera model 785 (JEOL USA, Inc., Peabody, MA)).

GNPOP was then synthesized using the seed-mediated growth procedure in the presence of CTAB. Briefly, 0.05 g of CTAB was dissolved in 45 mL of  $\text{H}_2\text{O}$  by sonication, and 2 mL of 0.01 M  $\text{HAuCl}_4 \cdot 3\text{H}_2\text{O}$  was then added under constant stirring. After stirring, 0.3 mL of 0.01 M  $\text{AgNO}_3$  was added to the solution and mixed properly. Consequently, 0.32 mL of 0.1 M ascorbic acid dropwise was added as a reducing agent. The solution turned from yellow to colorless. 0.5 mL of gold nano-popcorn seed was immediately added into the colorless solution and mixed for 2 min. The color changed to blue within 2 min, indicating the formation of popcorn nanostructures. To remove the extra CTAB in the reaction mixture solution, the freshly prepared GNPOP was rinsed several times with water and centrifuged at 4000rpm for 30min. Finally, the suspension was resuspended in sterile water with a final volume of 5 mL.

### Preparation and Characterization of Antibody-Modified GNPOPs

For selective sensing of MDR *Salmonella typhimurium DT104*, we modified the GNPOP surface with monoclonal antibody (mAb) M3038. Firstly, 80  $\mu\text{L}$  of  $10^{-4}$  M thiol ending polyethylene glycol (HOOC-PEG-SH) was added into 1 mL of GNPOPs mixture and stirred for 20 min at room temperature. The mixture was then stored at 4  $^\circ\text{C}$  overnight to allow the -SH group to bond with the GNPOPs while leaving a free carboxyl group at the other end. Excess HOOC-PEG-SH was removed by centrifugation at 4000 rpm for 1 h at room temperature (3 times). PBS was then added to achieve a final volume of 1 mL.

Secondly, covalent immobilization of the amine group of the antibody onto the carboxyl groups of PEG-SH was performed by ethyl-(dimethylaminopropyl)-carbodiimide (EDC) / N-hydroxysuccinimide (NHS) coupling catalysis. Briefly, 15  $\mu\text{L}$  of EDC (1 mg/mL) and 15  $\mu\text{L}$  of Sulfo-NHS (1 mg/mL) were first

added into 1.2 mL of the PEG-SH modified GNPOP solution, in order to form the amide bond to the carboxyl terminus of PEG on the SWCNTs-GNPOPs. A given amount of antibody was then added to the aforementioned solution. The solution was stirred for 2 min, and then stored for 2 h at room temperature, and another 12 h at 4  $^\circ\text{C}$ . The final GNPOPs-mAb suspension was centrifuged at 2,000 rpm for 10 min to remove any unbound antibodies. The residue was re-suspended in 5 mL of phosphate-buffered saline (PBS) solution and stored at 4  $^\circ\text{C}$  for use. This process was repeated for 3 times. The solution could be stored at 4  $^\circ\text{C}$  for at least 1 month.

### Bacteria Culture and Incubation with Antibody-Modified GNPOPs

*Salmonella typhimurium DT104*, *E. coli O157:H7* with resistance to ampicillin, chloramphenicol, streptomycin, sulfonamides, and tetracycline, were purchased from ATCC (ATCC 700408, ATCC 49979). The MDR bacteria were cultured by following the ATCC protocol as instructed. Initially, the supplied pellet of *DT104* was rehydrated on 5 to 6 mL Bacto™ Tryptic Soy Broth (TSB) and incubated at 37 $^\circ\text{C}$  for 24 h. Next, from the growth culture, a loop of bacteria was streaked on a tryptic agar plate and incubated for 24 h at 37 $^\circ\text{C}$ . A tryptic agar plate was made with Difco™ tryptic soy agar (TSA). A single colony from the TSA plate was inoculated into 10 mL TSB and incubated at 37  $^\circ\text{C}$  for 16 h in a shaker at 150 rpm, which resulted in an inoculum of  $10^8$  CFU/mL. All growth media were autoclaved at 121 $^\circ\text{C}$  for 15 min at high pressure (0.1 MPa) before the experiment. M3038-modified GNPOPs (20  $\mu\text{L}$ ) were added to 100  $\mu\text{L}$  of solution containing  $10-10^7$  CFU/mL of *Salmonella DT104*, suspended in 1 $\times$ PBS. The mixtures were incubated at room temperature for 20 min and were then washed 3 times with 1 $\times$ PBS buffer to make the final volume 100  $\mu\text{L}$ .

### Surface-Enhanced Raman Spectroscopy (SERS) for Targeted Sensing of *Salmonella*

A continuous wavelength diode-pumped solid-state laser (DPSS) laser operating at 670 nm was used as an excitation light source. We used InPhotonics 670 nm Raman fiber optic probe for excitation and data collection, with a 90 mm excitation fiber and 200 mm collection fiber. For Raman signal collection, a miniaturized QE65000 Scientific-grade Spectrometer from Ocean Optics was employed, with a response range of 220–3600  $\text{cm}^{-1}$ . The Hamamatsu FFT-CCD detector used in the QE65000 provides 90% quantum efficiency with high signal-to-noise and rapid signal processing speed as well as remarkable sensitivity for low-light level applications. The Raman spectrum was analyzed by Ocean Optics data acquisition SpectraSuite spectroscopy software.

### ICP-MS Analysis.

Finally, 100  $\mu\text{L}$  *Salmonella*-GNPOPs pellets were resuspended in a 900  $\mu\text{L}$  solution of 1%  $\text{HNO}_3$  with 1% BSA for digestion. The digested solution was introduced into the Varian 820 ICP-MS to detect Au at  $m/z$  197. For each sample and calibration solution, triplicate analyses were performed.

### Photothermal exposure and determination of live bacteria percentages

For photothermal destruction experiments, we applied a continuous wavelength laser (operating at 670 nm, with a power of 1 W  $\text{cm}^{-2}$  as an excitation light source) to our GNPOP-bacteria hybrids for 5–30 min. Then, the bacteria were transferred to tryptic agar plate after

photothermal destruction, which was incubated for 24 h at 37°C. The colony number for each countable plate was then counted with a colony counter. For accuracy, each experiment was performed 3 times.

### 3. Results and discussion

We synthesized gold nanoparticles through a two-step process, using seed-mediated growth. Transmission electron microscopy and UV-visible absorption spectroscopy were used to characterize the nanoparticles, as shown in Figure 2. TEM images showed the size of GNPOPs is around 40-50 nm, which was in accordance with DLS data (Figure 2B). Similar to spherical gold nanoparticles, GNPOPs has one plasmon band in UV. However, its  $\lambda$  max was shifted about 60 nm in comparison to that of a spherical gold nanoparticle (GNP) of the same size (Figure 2C).

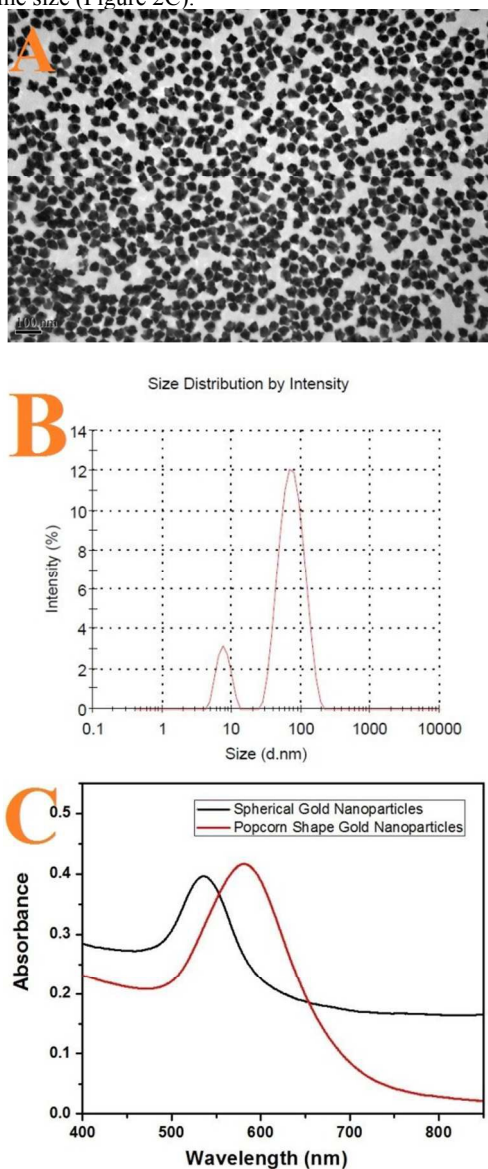


**Figure 2.** (A) TEM image showing freshly prepared GNPOPs. (B) DLS analysis of GNPOP size distribution. (C) UV Spectroscopy Absorption spectra showing absorbance for only GNPOP compared with round shaped gold nanoparticle.

We performed ICP-MS to measure the concentration of  $\text{Au}^{3+}$  in the final 5 mL GNPOP. The experimental value was  $3.87 \times 10^{-3}$  mol/L with a yield around 97%. To measure how many Au atoms in one GNPOP, we designed a method by calibrating the number of GNPOPs against the concentration of  $\text{Au}^{3+}$  in solution. For easy calculation of the number of GNPOPs, we used SWCNT with a -SH group to concentrate the GNPOPs because the -SH group can bind well with GNPOPs. In detail, we diluted 1  $\mu\text{L}$  GNPOPs to 10 mL, and added it to several amounts of the functionalized SWCNTs and continued stirring for 1 h. After binding, we diluted 1  $\mu\text{L}$  of the hybrid nanoparticle into 10 mL again, and then we checked the 6  $\mu\text{L}$  solution via TEM (Figure 3). We observed that almost all of the GNPOPs bind with SWCNTs, and then we calculated the number of the GNPOPs, and repeated this procedure 10 times. An average of 70-80 GNPOPs were in 6  $\mu\text{L}$  of SWCNTs-GNPOPs solution. Thus, the amount of Au atoms in each GNPOP was determined. Our results showed that each GNPOP (45 nm size) had around  $2 \times 10^6$  Au atoms.

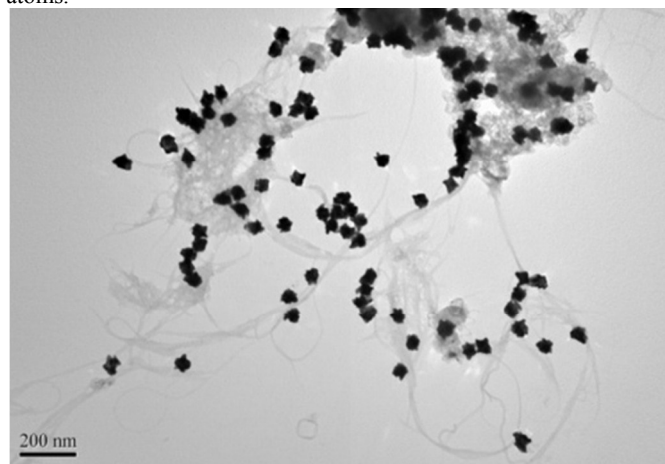


**Figure 3.** TEM image showing GNPOPs-decorated SWCNTs. A concentrated GNPOP sample was achieved through GNPOPs-SWCNT binding.

To avoid nonspecific binding with bacteria, GNPOPs were coated with thiolated polyethylene glycol (HS-PEG), which provided a carboxyl group for binding with a monoclonal antibody. Results showed that PEG-SH coated GNPOPs weren't binding with both *Salmonella DT104* and *E.Coli O157:H7* (Figure 4). Characterization of mAb conjugated GNPOPs was performed with DLS measurements. GNPOPs have an average size of 44 nm, which was also confirmed by TEM data. The addition of mAb to the GNPOPs changed the diameter to 49 nm. This is expected because the mAb size was around 3 nm, leading to an increased total diameter by 5-6 nm. The UV max was slight red shifted to 590 nm due to the coating (Figure 5D). The pH of GNPOP-PEG was 8.5, with a zeta potential of 55-60, indicating a highly stable and dispersed solution.<sup>76</sup>

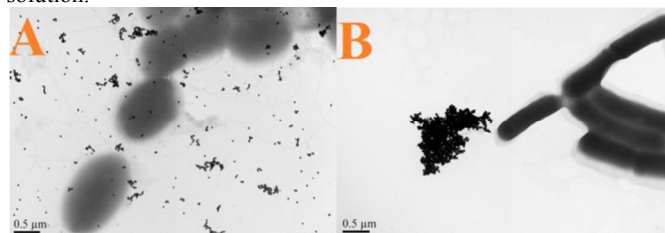


**Figure 4.** TEM image showing no GNPOP binding with any kind of bacteria after the coating with PEG-SH. (A) *Salmonella DT104*. (B) *E.Coli O157:H7*.

To accurately measure the number of antibody molecules in each GNPOP, we performed a KCN dissolution procedure followed by fluorescence analysis. First, we treated the Cy3-labeled antibody conjugated GNPOP with 10  $\mu$ M potassium cyanide to oxidize them. After that, the solution containing the released Cy3-labeled antibody was collected for fluorescence analysis. The amount of Cy3-labeled antibody was measured by fluorescence. By dividing the total number of Cy3-labeled antibody by the total number of GNPOPs, we estimated that there were about 30-40 antibody per GNPOP.

Our results suggested that newly formed GNPOP-PEGSH-mAb could specifically bind with *Salmonella DT104* (Figure 5A). On the contrary, there was no specificity with *Salmonella Agona* and *E. Coli* (Figure 5B&C). Data from UV spectroscopy showed red shift with the modification of mAb and a broader peak with *Salmonella* (Figure 5D). There are two possible reasons for the red shift: firstly, the change in the local refractive index on the GNPOP's surface caused by specific binding of the mAb on GNPOPs; secondly the interparticle interaction resulting from the assembly of nanoparticles on the surface of the bacteria.

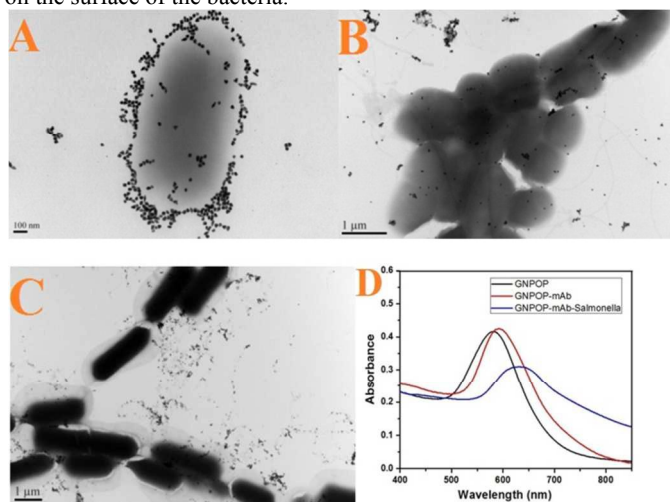


**Figure 5.** (A) TEM image showing that antibody conjugated GNPOPs adsorbed onto *Salmonella DT104*. (B) TEM image showing that antibody conjugated GNPOPs did not attach onto *Salmonella Agona*. (C) TEM image showing that antibody conjugated GNPOPs had no specific binding with *E. Coli O157:H7*. (D) UV absorption spectra of GNPOPs, GNPOP-mAb, and GNPOP-mAb-*Salmonella*.

In addition, SERS was performed to potentially establish a fast detection method for *Salmonella* in real samples. The central sphere of GNPOP served as an electron reservoir while the tips were capable of focusing the field at their apexes, which provided sufficient field of enhancement of the scattering signal. As a result, low cross-section Raman signals could be amplified by several orders of magnitude using GNPOP, particularly in narrow nanoscaled spikes and edges. In the presence of drug resistant MDRB *Salmonella DT104* as low as 5 CFU/mL, antibody-conjugated GNPOPs could adsorb onto the bacterial cell wall. Consequently, they formed several hot spots to provide a significant enhancement of the Raman signal intensity of Rh6G modified monoclonal M3038 antibodies through electromagnetic field enhancements (Figure 6). However, the change of SERS intensity was negligible in the presence of *Salmonella Agona* and *E. Coli O157:H7*. This might be mainly due to the lack of strong interaction between mAb-conjugated GNPOPs and *Salmonella Agona* or *E. coli* bacteria.

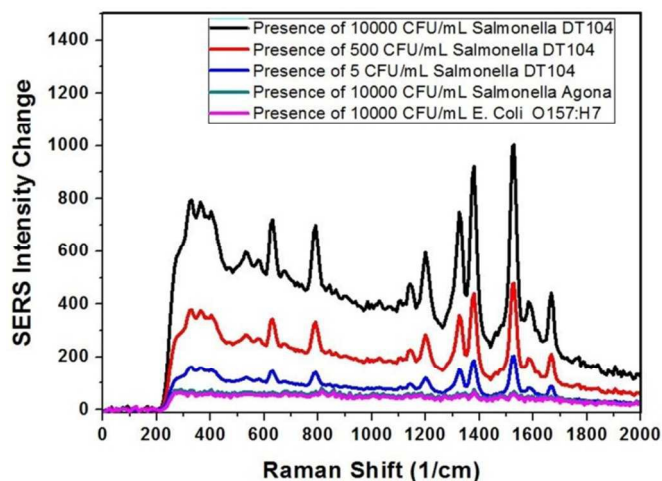


**Figure 6.** SERS enhancement (SERS intensity change before and after addition of bacteria) caused by the addition of different concentrations *Salmonella DT104* to monoclonal M3038 antibody-conjugated GNPOPs.

ICP-MS was used for the detection of *Salmonella DT104* under the assumption that each *Salmonella* bonds with the same amount of GNPOPs in certain concentrations. Thus, ICP-MS could be the most sensitive and effective way to detect GNPOP-bonded *Salmonella DT104*. In order to avoid false results, centrifugation was used to separate GNPOP-bonded *Salmonella DT104* and free GNPOPs. Our results indicated that centrifugation for 20 min at 2000 rpm was optimal for fulfilling this purpose. The bacteria concentration was also confirmed by bacteria colony counting. As shown in Figure 7, there were no bacteria remaining in the supernatant, indicating the successful separation of bacteria. Moreover, the absence of free GNPOP in the pellet from centrifugation was confirmed by using TEM and UV-Vis spectroscopy. Another centrifugation was performed, and 1 mL of the supernatant was examined by ICP-MS. Data showed a concentration of 100 ppq for  $Au^{3+}$ , suggesting 100-150 free GNPOPs per mL. This tiny amount of GNPOPs could be negligible.

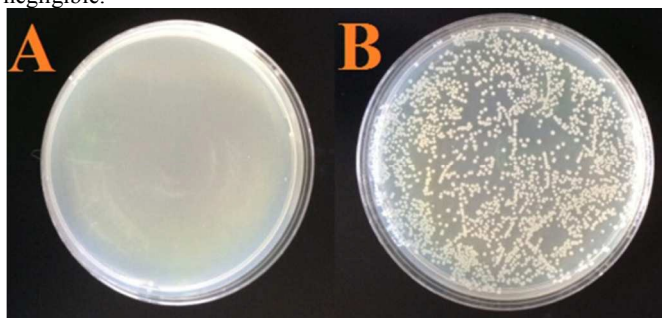


**Figure 7.** Colonies of *Salmonella DT104*. (A) Colonies shows the absence of bacteria in the supernatant solution after centrifugation. (B) Colonies show the presence of *Salmonella DT104* in the suspension of GNPOPs conjugated *Salmonella DT104* after centrifugation and resuspension in PBS.

To carry out an analysis of the concentration of bacteria, an extra amount of the antibody-conjugated GNPOPs were added to a sample solution. The utilization of antibodies afforded a feasible way to specifically connect the bacteria cells and GNPOPs. After the mixture was centrifuged to separate the free GNPOPs from the mixture, GNPOPs bonded *Salmonella* was then acid-digested and the concentration of  $Au^{3+}$  was quantified using ICP-MS. Standard

curves were produced to correlate the concentration of *Salmonella* DT104 and the concentration of  $\text{Au}^{3+}$ . In the meantime, by determining the concentration of  $\text{Au}^{3+}$  versus the concentration of *Salmonella*, the amount of GNPOPs (or in the form of  $\text{Au}^{3+}$ ) could be correlated with each CFU of *Salmonella*. Figure 8 indicated a close relationship between the concentration of  $\text{Au}^{3+}$  and the typical results from one set of experiments with different concentrations of *Salmonella* where a linear correlation of 0.966 ( $R^2$ ), ranging from  $10^1$  to  $10^7$  CFU/mL, was obtained. The signal intensity increases with increasing bacteria concentrations, and a detection limit of 100 CFU/mL was achieved. This conservative estimate was based on three times the standard deviation of the background plus the mean blank values from triplicate analyses of each of the 6 blanks. The linear dynamic range was between  $10^2$  and  $10^5$  CFU/mL with a linear correlation  $R^2 = 0.9902$ .

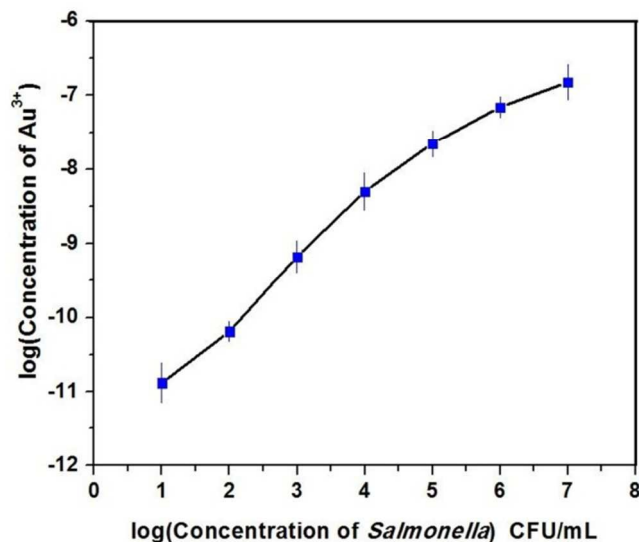


**Figure 8.** Standard curve showing the relationship between the concentration of *Salmonella* and the ICP-MS signal of  $\text{Au}^{3+}$ .

The signal intensities of  $\text{Au}^{3+}$  increased with the increased concentration of *Salmonella*, but these  $\text{Au}^{3+}$  signal intensities were slightly nonlinear over the high concentration range (Figure 8). We suspected that the nonlinearity observed at the high bacterial concentrations could be due to bacterial aggregation (Figure 9) which reduces the cell surface area for binding to the antibody. As we have mentioned, there were 30-40 mAbs conjugated with each GNPOP. The adsorption of mAbs conjugated GNPOPs onto *Salmonella* could lead to bacterial aggregation, resulting in the decrease of their surface area available for binding with more antibody-conjugated GNPOPs. Consequently, signals of  $\text{Au}^{3+}$  might be lower than expected for a high concentration of bacteria. As shown in Figure 8, the bacteria concentration increased from  $10^1$  to  $10^7$  CFU/mL, meanwhile the amount of GNPOPs bound to each CFU decreased from 4000 to 100, respectively. This suggests that our assay could be more useful for detecting low concentrations of bacterial pathogens.

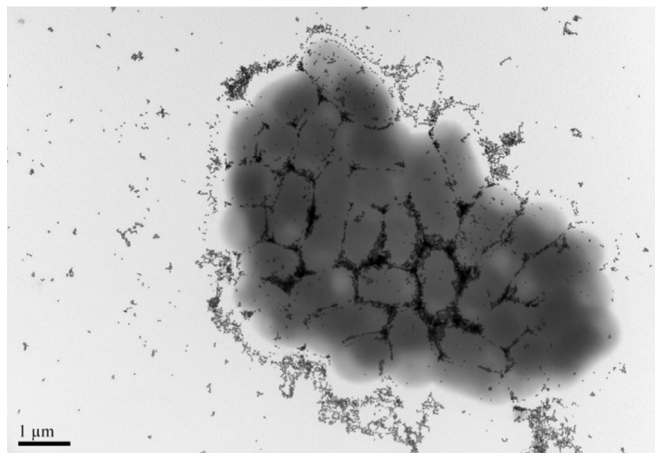


**Figure 9.** TEM image showing *Salmonella* aggregation at high bacterial concentrations, which gave rise to a nonlinear relationship between the ICP-MS signals for the concentration of *Salmonella* and  $\text{Au}^{3+}$ .

Our assay included the following techniques: incubation of *Salmonella* with mAb-GNPOPs, centrifugation to isolate and purify the nano-hybrids, acid digestion, and ICP-MS analysis. Since *Salmonella* labeling and ICP-MS analysis require only minimum sample preparation, our assay is easy and fast, normally less than 40 min for each test (20 min for incubation, 15 min for washing and acid digestion, and 5 min for ICP-MS analysis). Triple ICP-MS analyses showed a low relative standard deviation (RSD) of 5%, while triple sample preparations exhibited a RSD of 10%.

To assess the photothermal efficiency of our nano-hybrid system toward the eradication of *Salmonella*, a  $1 \text{ W/cm}^2$  670 nm light source was used. Noticeably, the conjugation of *Salmonella* with GNPOPs caused a maximum absorbance red shift to 630 nm. Thus a 670 nm light source is sufficient for our purpose. A full amount of mAb conjugated GNPOPs was added to bind with *Salmonella*. Centrifugation was then used to remove the free mAb conjugated GNPOPs. As indicated in Figure 10, laser irradiation time was dependent on the concentration of bacteria (CFU/mL), indicating a close correlation to the mortality of *Salmonella*. Our results demonstrated that our photothermal destruction with monoclonal M3038 antibody-conjugated GNPOPs could eliminate almost 100% of *Salmonella* within 19 min, at a bacterial concentration of  $10^5$  CFU/mL. Furthermore, our data also suggest that almost 100% of bacteria can be destroyed in 6 to 30 minutes of laser irradiation treatment, depending on its concentration ( $10^2$ – $10^7$  CFU/mL).

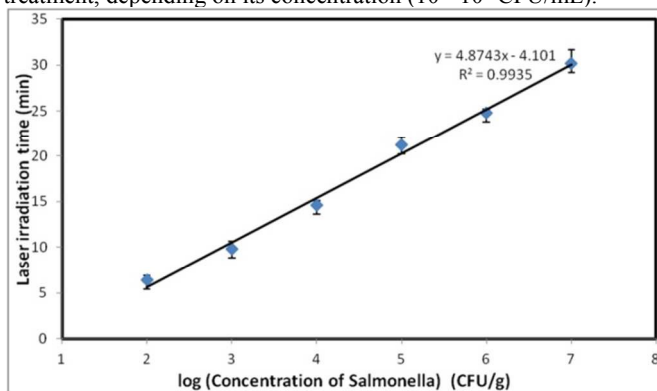


**Figure 10.** Plot showing laser irradiation time to kill almost 100% of *Salmonella* DT104 at different concentrations.

Data analysis indicated that the viability of *Salmonella* at a concentration of  $10^5$  CFU/mL was related to the laser exposure time within 30 min (Figure 11) after adding the calculated amount of GNPOPs. It is noted that the exposure of *Salmonella*-GNPOPs conjugates to the laser could eliminate most of the *Salmonella* within 20 min. However, cell viability was more than 93% in the testing group of *S. Agona* and *E. Coli*. This in turn evidenced that the conjugation of GNPOPs with bacteria is crucial for effective photothermal destruction. *Salmonella DT104* conjugated with GNPOPs exhibited a strong absorption at the excitation wavelength of 600 nm (Figure 5). Considering the application of our thermal therapy in a clinical setting, it is necessary to elucidate the effect of the extra amount of GNPOPs because the total removal of GNPOPs may not always be accomplished. For our next set of experiments, we used a concentration of bacteria at  $10^5$  CFU/mL, and the amount of GNPOPs also played an important role in eliminating bacteria. As shown in Figure 10, it took 27 min to eliminate all bacteria with the calculated amount of GNPOPs. However, the photothermal time could be reduced to 25 min, 20 min, and 19 min, with 5%, 30%, and 50% more GNPOP than calculated, respectively. Interestingly, there was no similar effect when using additional amounts of GNPOPs whereby 100%, 200%, and even 1000% more than calculated amount were used. The possible reason for this direct correlation up to 50% is that, since the heat produced by GNPOP is very localized, for the small extra amount of GNPOPs added, the photo thermal effect might be enhanced due to the saturated binding resulting from more available GNPOPs. The binding of GNPOPs with bacteria reached saturation when a 100% more GNPOPs were added, resulting in no further enhancement of photothermal therapy.

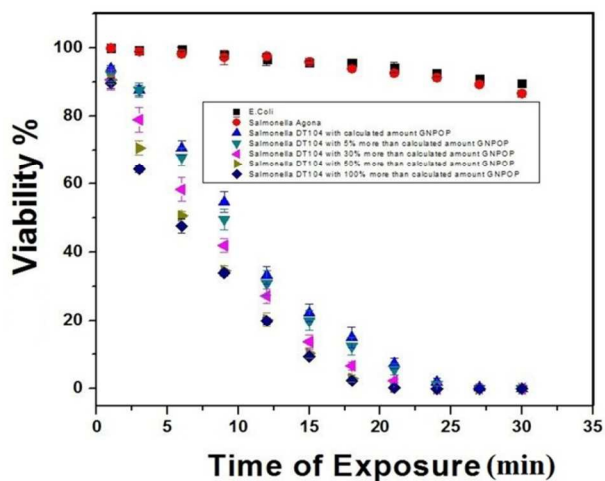


**Figure 11.** A plot showing bacteria viability measurements when mAb attached GNPOP conjugated with *E. Coli*, *Salmonella Agona*, and *Salmonella DT104* with different concentrations GNPOPs of using  $1 \text{ W/cm}^2$  670 nm light for 30 min.

It is noted that an extra amount of more than 100% of GNPOPs added had not only no further benefit towards photothermal destruction, but also, considerable destruction to its surrounding normal cells in the long run. As shown in Figure 12, the supplement of GNPOPs could result in considerable toxicity towards HaCat cells in a dose-dependent manner. It is clear that the GNPOPs exhibited low toxicity towards HaCat cells in the first few hours (5h). However, as the concentration of GNPOPs was increased to correspond to 100% more than the calculated amount (around  $1.33 \times 10^8$  /mL) for  $10^5$  CFU/mL, the toxicity of GNPOP was observed. The possible reason for the toxicity may result from the

free CTAB. Even though we enclosed the GNPOP with PEG-SH to reduce potential CTAB toxicity, the self-aggregated extra unbound GNPOPs may cause some CTAB detachment from the particle, thus introducing cytotoxicity.<sup>77-79</sup> With the consideration of the photothermal efficiency and cytotoxicity, 30-50% more than the calculated amount of GNPOPs can be considered as the best choice.

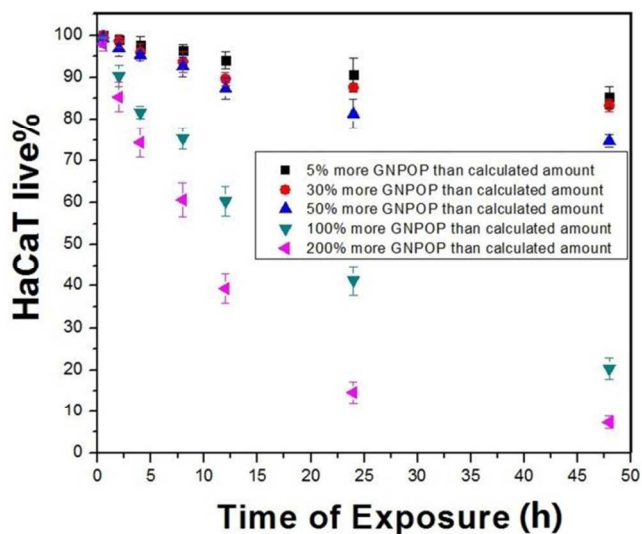


**Figure 12.** Plot showing HaCat Cell viability measurements where  $1 \text{ W/cm}^2$  670 nm light was used for 15 min with differing concentrations of GNPOPs.

To further investigate the photothermal performance of our GNPOP, we performed the same photo thermal experiment with multifunctional gold nanorods (GNR) and spherical gold nanoparticles (GNP) using  $1 \text{ W/cm}^2$  670 nm NIR continuous-wave radiation. The photothermal effect of our GNPOPs was more profound than the other two shapes of GNPs. One of the possible reasons is that the laser frequency was close to the maximum absorbance of GNPOPs than GNP and GNR, resulting in higher photo thermal efficiency. Another possible reason was that several narrow, nanoscale sharp tips were capable of focusing the field at their apexes, which could provide considerable enhancement of photothermal efficiency. Ultimately, when exposed to our source of laser irradiation GNPOPs acted as better heat producers than the other shapes that were attached. Furthermore, in order to understand how the temperatures changed during photo thermal destruction, we performed thermal imaging at one minute intervals during the photothermal experiments by using a MikroShot Camera. We found that the temperature increased to  $48^\circ\text{C}$  when nanoparticle-bound MDR *Salmonella DT104* were exposed to a 670 nm laser with  $1 \text{ W/cm}^2$  power for 10 min. Conversely, under the same conditions, the temperature increased to only  $30^\circ\text{C}$  for *E. coli* without any nanoparticles.

#### 4. Conclusions

In conclusion, we have developed a new method to detect and measure *Salmonella DT104* by using GNPOPs labeling, Raman spectroscopy and ICP-MS, which can also be used for quantitative photothermal destruction. For qualitative analysis, we have shown that antibody-conjugated hybrid nanomaterials can provide a significant enhancement of the Raman signal intensity by several orders of magnitude in the presence of *Salmonella DT104*. TEM

images of *Salmonella* and *E. coli* clearly demonstrate that our SERS assay is highly sensitive in detecting *Salmonella DT104* through antibody–antigen recognition. For quantitative analysis, our assay can measure an extremely low concentration of *Salmonella DT104* at 100 CFU/mL. However, the accuracy of our assay may be reduced when a high concentration of bacteria is used ( $>10^5$  CFU/mL), owing to the decrease of the bacteria's surface area available for binding to the antibody-conjugated GNPOPs resulting from the aggregation of the *Salmonella*. For photothermal destruction, our experimental results show that the localized heating of antibody conjugated GNPOPs at 670 nm light irradiation for 20 min ( $1 \text{ W/cm}^2$ ) can lead to irreversible cellular-damage and eliminate almost 100% of MDR *Salmonella* bacteria at the concentration of  $10^5$  CFU/mL. Noticeably, an extra amount of 50% more GNPOPs than calculated may be toxic to normal cells with our proposed photothermal therapy. With the consideration of the photothermal efficiency and cytotoxicity, 30–50% more than the calculated amount of GNPOPs should be used as a balanced choice. We believe that our assay has the potential to be utilized for the high-throughput screening of MDR bacteria, and can be developed as an effective assay for rapid detection of bacterial pathogens and photothermal destruction in non-laboratory settings. Finally, the feasibility demonstrated here for the analysis of *Salmonella DT104* suggests the potential of similar immunoassays for a wide variety of bacterial or other pathogens.

#### ACKNOWLEDGMENT

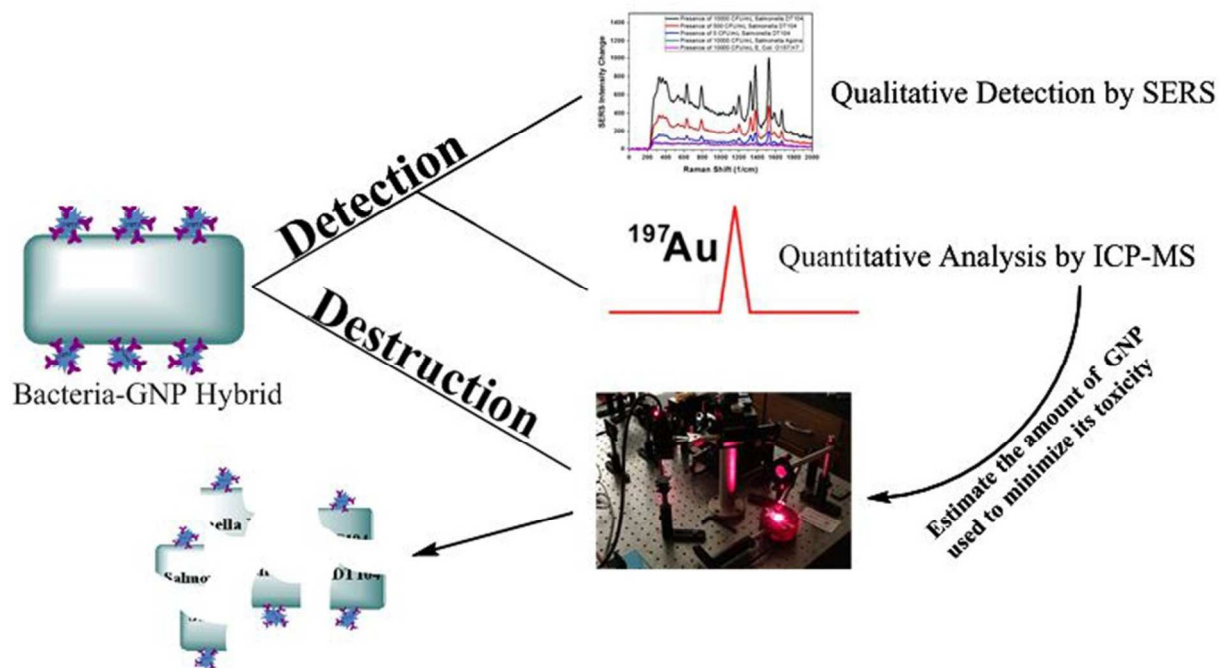
The project was supported by the National Science Foundation (HBCU-RISE: HRD-1137763 and PREM: DMR-1205194). The TEM CORE facilities were supported by the National Institutes of Health/ National Center for Research Resources (Award Number: G12RR013459) and the National Institutes of Health /National Institute on Minority Health and Health Disparities (Award Number: G12MD007581).

#### Notes and references

- <http://www.cdc.gov/foodborneburden/>.
- <http://www.cdc.gov/fmo/topic/Budget%20Information/index.html>2010.
- <http://www.cdc.gov/salmonella/>.
- <http://www.cdc.gov/media/releases/2014/p0326-salmonella-data.html>.
- A. T. Hamme II, Y. Lin. and T. J. O., *Food Poisoning: Outbreaks, Bacterial Sources and Adverse Health Effects*, 2014, 213-238.
- S. Eckhardt, P. S. Brunetto, J. Gagnon, M. Priebe, B. Giese and K. M. Fromm, *Chemical reviews*, 2013, 113, 4708-4754.
- S. A. Svarovsky and M. J. Gonzalez-Moa, *ACS combinatorial science*, 2011, 13, 634-638.
- M. M. Hoehl, P. J. Lu, P. A. Sims and A. H. Slocum, *Journal of agricultural and food chemistry*, 2012, 60, 6349-6358.
- R. T. N. a. S. B. Weisberg, *Journal of Water and Health*, 2005, DOI: 10.2166/wh.2005.051.
- N. Duan, S. Wu, X. Chen, Y. Huang, Y. Xia, X. Ma and Z. Wang, *Journal of agricultural and food chemistry*, 2013, 61, 3229-3234.
- J. Sundaram, B. Park, A. Hinton, Jr., S. C. Yoon, W. R. Windham and K. C. Lawrence, *Journal of agricultural and food chemistry*, 2012, 60, 991-1004.
- W. Wu, J. Li, D. Pan, J. Li, S. Song, M. Rong, Z. Li, J. Gao and J. Lu, *ACS applied materials & interfaces*, 2014, 6, 16974-16981.
- P. S. Annie Rompre, Julia Baudart, Marie-Rene'e de-Roubin, Patrick Laurent, *Journal of Microbiological Methods*, 2002, 31-54.
- M. J. Chapela, P. Fajardo, A. Garrido, A. G. Cabado, M. Ferreira, J. Lago and J. M. Vieites, *Journal of agricultural and food chemistry*, 2010, 58, 4051-4055.
- Z. Y. Yang, W. B. Shim, K. Y. Kim and D. H. Chung, *Journal of agricultural and food chemistry*, 2010, 58, 7135-7140.
- L. R. Shen, S. Dilireba, W. X. Zhou, Y. R. Wang, M. L. Li and L. Zhai, *Journal of agricultural and food chemistry*, 2014, 62, 9305-9309.
- N. Schneider, I. Weigel, K. Werkmeister and M. Pischetsrieder, *Journal of agricultural and food chemistry*, 2010, 58, 76-81.
- A. M. Hamid, A. K. Jarmusch, V. Pirro, D. H. Pincus, B. G. Clay, G. Gervasi and R. G. Cooks, *Analytical chemistry*, 2014, 86, 7500-7507.
- M. A. Burkin and I. A. Galvidis, *Journal of agricultural and food chemistry*, 2010, 58, 9893-9898.
- S. A. H. Blake Farrow, Errika C. Romero, Bert Lai, Matthew B. Coppock, Kaycie M. Deyle, Amethyst S. Finch, Dimitra N. Stratis-Cullum, Heather D. Agnew, Sung Yang, and James R. Heath, *ACS Nano*, 2013, 7, 9452-9460.
- A. Costantini, E. Vaudano, V. Del Prete, M. Danei and E. Garcia-Moruno, *Journal of agricultural and food chemistry*, 2009, 57, 10664-10669.
- O. C. Shanks, M. Sivaganesan, L. Peed, C. A. Kelty, A. D. Blackwood, M. R. Greene, R. T. Noble, R. N. Bushon, E. A. Stelzer, J. Kinzelman, T. Anan'eva, C. Sinigalliano, D. Wanless, J. Griffith, Y. Cao, S. Weisberg, V. J. Harwood, C. Staley, K. H. Oshima, M. Varma and R. A. Haugland, *Environmental science & technology*, 2012, 46, 945-953.
- J. P. G. Shana Topp, *J. AM. CHEM. SOC.*, 2007, 129, 6807-6811.
- J. Borrero, Y. Chen, G. M. Dunny and Y. N. Kaznessis, *ACS synthetic biology*, 2014, DOI: 10.1021/sb500090b.
- Z. Hosseinidoust, T. G. Van de Ven and N. Tufenkji, *Langmuir : the ACS journal of surfaces and colloids*, 2011, 27, 5472-5480.
- S. T. Lee, D. Cook, J. A. Pfister, J. G. Allen, S. M. Colegate, F. Riet-Correa and C. M. Taylor, *Journal of agricultural and food chemistry*, 2014, 62, 7345-7354.
- M. S. Kim, Y. S. Yoon, J. G. Seo, H. G. Lee, M. J. Chung and D. Y. Yum, *Toxicological research*, 2013, 29, 129-135.
- R. L. Santos, S. Zhang, R. M. Tsolis, R. A. Kingsley, L. Garry Adams and A. J. Bäumlner, *Microbes and Infection*, 2001, 3, 1335-1344.
- P. Mastroeni and M. Sheppard, *Microbes and Infection*, 2004, 6, 398-405.
- J. Davies and D. Davies, *Microbiology and molecular biology reviews : MMBR*, 2010, 74, 417-433.
- F. Baquero, J.-L. Martinez and R. Cantón, *Current Opinion in Biotechnology*, 2008, 19, 260-265.
- J. W. Costerton, P. S. Stewart and E. P. Greenberg, *Science*, 1999, 284, 1318-1322.
- B. G. Spratt, *Proceedings of the National Academy of Sciences*, 1975, 72, 2999-3003.
- S. Caras and J. Janata, *Analytical chemistry*, 1980, 52, 1935-1937.
- B. G. Spratt and A. B. Pardee, *Nature*, 1975, 254, 516-517.
- H. J. Duggleby, S. P. Tolley, C. P. Hill, E. J. Dodson, G. Dodson and P. C. E. Moody, *Nature*, 1995, 373, 264-268.
- G. D. Wright, *Chemical Communications*, 2011, 47, 4055-4061.
- P. C. Ray, S. A. Khan, A. K. Singh, D. Senapati and Z. Fan, *Chemical Society Reviews*, 2012, 41, 3193-3209.
- J. Davies and D. Davies, *Microbiology and Molecular Biology Reviews*, 2010, 74, 417-433.
- R. Nery, in *Cancer*, Springer US, 1986, DOI: 10.1007/978-1-4684-8091-7\_3, ch. 3, pp. 83-137.
- H. Font, J. Adrian, R. Galve, M. C. Estévez, M. Castellari, M. Gratacós-Cubarsí, F. Sánchez-Baeza and M. P. Marco, *Journal of agricultural and food chemistry*, 2008, 56, 736-743.
- S. Fitting, S. Zou, W. Chen, P. Vo, K. F. Hauser and P. E. Knapp, *Journal of Proteome Research*, 2010, 9, 1795-1804.
- L.-L. Li, J.-H. Xu, G.-B. Qi, X. Zhao, F. Yu and H. Wang, *ACS Nano*, 2014, 8, 4975-4983.
- Y. Lin and A. T. Hamme II, *Analyst*, 2014, 139, 3702-3705.
- A. M. Gobin, M. H. Lee, N. J. Halas, W. D. James, R. A. Drezek and J. L. West, *Nano Letters*, 2007, 7, 1929-1934.
- L. Tong, Q. Wei, A. Wei and J.-X. Cheng, *Photochemistry and Photobiology*, 2009, 85, 21-32.
- P. K. Jain, X. Huang, I. H. El-Sayed and M. A. El-Sayed, *Accounts of Chemical Research*, 2008, 41, 1578-1586.
- T. J. Ondera and A. T. Hamme II, *Journal of Materials Chemistry B*, 2014, 2, 7534-7543.

49. X. Dai, Z. Fan, Y. Lu and P. C. Ray, *ACS applied materials & interfaces*, 2013, 5, 11348-11354.
50. W. Huang, J. Giddens, S.-Q. Fan, C. Toonstra and L.-X. Wang, *Journal of the American Chemical Society*, 2012, 134, 12308-12318.
51. B. M. DeRussy, M. A. Aylward, Z. Fan, P. C. Ray and R. Tandon, *Sci. Rep.*, 2014, 4.
52. S. Zhang, Y. Moustafa and Q. Huo, *ACS applied materials & interfaces*, 2014, 6, 21184-21192.
53. W. Jiang, R. Yuan, Y. Chai, L. Mao and H. Su, *Biosensors and Bioelectronics*, 2011, 26, 2786-2790.
54. J. Gao, X. Huang, H. Liu, F. Zan and J. Ren, *Langmuir : the ACS journal of surfaces and colloids*, 2012, 28, 4464-4471.
55. H. Y. Tsai, C. F. Hsu, I. W. Chiu and C. B. Fuh, *Analytical chemistry*, 2007, 79, 8416-8419.
56. H. Park, S. Lee, L. Chen, E. K. Lee, S. Y. Shin, Y. H. Lee, S. W. Son, C. H. Oh, J. M. Song, S. H. Kang and J. Choo, *Physical Chemistry Chemical Physics*, 2009, 11, 7444-7449.
57. G. Saito, J. A. Swanson and K.-D. Lee, *Advanced Drug Delivery Reviews*, 2003, 55, 199-215.
58. A. Wolcott, D. Gerion, M. Visconte, J. Sun, A. Schwartzberg, S. Chen and J. Z. Zhang, *The Journal of Physical Chemistry B*, 2006, 110, 5779-5789.
59. H. Tang, J. Chen, L. Nie, Y. Kuang and S. Yao, *Biosensors and Bioelectronics*, 2007, 22, 1061-1067.
60. Z. Fan, D. Senapati, S. A. Khan, A. K. Singh, A. Hamme, B. Yust, D. Sardar and P. C. Ray, *Chemistry – A European Journal*, 2013, 19, 2839-2847.
61. J. Chen, D. Wang, J. Xi, L. Au, A. Siekkinen, A. Warsen, Z.-Y. Li, H. Zhang, Y. Xia and X. Li, *Nano Letters*, 2007, 7, 1318-1322.
62. Y.-F. Huang, K. Sefah, S. Bamrungsap, H.-T. Chang and W. Tan, *Langmuir : the ACS journal of surfaces and colloids*, 2008, 24, 11860-11865.
63. D. Pissuwan, C. H. Cortie, S. M. Valenzuela and M. B. Cortie, *Trends in Biotechnology*, 2010, 28, 207-213.
64. K. Vanherck, S. Hermans, T. Verbiest and I. Vankelecom, *Journal of Materials Chemistry*, 2011, 21, 6079-6087.
65. H. Yuan, S. Gao, X. Liu, H. Li, D. Günther and F. Wu, *Geostandards and Geoanalytical Research*, 2004, 28, 353-370.
66. S. E. Jackson, N. J. Pearson, W. L. Griffin and E. A. Belousova, *Chemical Geology*, 2004, 211, 47-69.
67. G. A. Jenner, H. P. Longrich, S. E. Jackson and B. J. Fryer, *Chemical Geology*, 1990, 83, 133-148.
68. J. S. Becker, M. Zoriy, A. Matusch, B. Wu, D. Salber, C. Palm and J. S. Becker, *Mass Spectrometry Reviews*, 2010, 29, 156-175.
69. F. Chainet, C.-P. Lienemann, J. Ponthus, C. Pécuyer, J. Castro, E. Tessier and O. F. X. Donard, *Spectrochimica Acta Part B: Atomic Spectroscopy*, 2014, 97, 49-56.
70. E. Song, W. Han, J. Li, Y. Jiang, D. Cheng, Y. Song, P. Zhang and W. Tan, *Analytical chemistry*, 2014, 86, 9434-9442.
71. Y. Luo, X. Yan, Y. Huang, R. Wen, Z. Li, L. Yang, C. J. Yang and Q. Wang, *Analytical chemistry*, 2013, 85, 9428-9432.
72. L. Beqa, Z. Fan, A. K. Singh, D. Senapati and P. C. Ray, *ACS applied materials & interfaces*, 2011, 3, 3316-3324.
73. R. M. Stöckle, Y. D. Suh, V. Deckert and R. Zenobi, *Chemical Physics Letters*, 2000, 318, 131-136.
74. S. Muyldermans, C. Cambillau and L. Wyns, *Trends in Biochemical Sciences*, 2001, 26, 230-235.
75. A. Maiti, A. Maiti, P. Das, D. Senapati and T. Kumar Chini, *ACS Photonics*, 2014, 1, 1290-1297.
76. [http://en.wikipedia.org/wiki/Zeta\\_potential](http://en.wikipedia.org/wiki/Zeta_potential).
77. M. Tarantola, A. Pietuch, D. Schneider, J. Rother, E. Sunnick, C. Rosman, S. Pierrat, C. Sönnichsen, J. Wegener and A. Janshoff, *Nanotoxicology*, 2011, 5, 254-268.
78. E. Boisselier and D. Astruc, *Chemical Society Reviews*, 2009, 38, 1759-1782.
79. P. Rivera-Gil, D. Jimenez De Aberasturi, V. Wulf, B. Pelaz, P. Del Pino, Y. Zhao, J. M. De La Fuente, I. Ruiz De Larramendi, T. Rojo, X.-J. Liang and W. J. Parak, *Accounts of Chemical Research*, 2012, 46, 743-749.

# Table of Contents



We developed a GNP labeling based assay to measure the concentration of *bacteria* and to guide its quantitative photothermal destruction.